HHS Public Access

Author manuscript

Nat Med. Author manuscript; available in PMC 2011 July 01.

Published in final edited form as:

Nat Med. 2011 January ; 17(1): 96–104. doi:10.1038/nm.2270.

Desmoglein 2 is a receptor for adenovirus serotypes 3, 7, 11, and 14

Hongjie Wang[1,2], **ZongYi Li**[1], **Ying Liu**[1], **Jonas Persson**[1], **Ines Beyer**[1], **Thomas Möller**[3], **Dilara Koyuncu**[4], **Max R. Drescher**[1], **Robert Strauss**[1], **Xiao-Bing Zhang**[5], **James K. Wahl III**[6], **Nicole Urban**[7], **Charles Drescher**[7], **Akseli Hemminki**[2], **Pascal Fender**[8], and **André Lieber**[1]

[1]University of Washington, Division of Medical Genetics, Box 357720, Seattle, WA 98195 [2]Cancer Gene Therapy Group, University of Helsinki & Helsinki University Central Hospital, Helsinki, Finland [3]University of Washington, Department of Neurology [4]Bogazici University, Department Molecular Biology and Genetics, Istanbul, Turkey [5]Loma Linda University, Department of Medicine, Division of Regenerative Medicine Loma, Linda, CA 92350 [6]University of Nebraska Medical Center, Omaha, Nebaska [7]Fred Hutchinson Cancer Research Center, Seattle, WA [8]Unit of Virus Host Cell Interactions, Grenoble, France

Abstract

We have identified desmoglein 2 (DSG2) as the primary high-affinity receptor used by adenovirus (Ad) serotypes Ad3, Ad7, Ad11, and Ad14. These serotypes represent important human pathogens causing respiratory tract infections. In epithelial cells, adenovirus binding to DSG2 triggers events reminiscent of epithelial-to-mesenchymal transition, leading to transient opening of intercellular junctions. This improves access to receptors, e.g. CD46 and Her2/*neu*, that are trapped in intercellular junctions. In addition to complete virions, dodecahedral particles (PtDd), formed by viral penton and fiber in excess during viral replication, can trigger DSG2-mediated opening of intercellular junctions as shown by studies with recombinant Ad3 PtDd. Our findings shed light on adenovirus biology and pathogenesis and have implications for cancer therapy.

Introduction

Human adenoviruses (Ads) have been classified into six species (A to F) currently containing 55 serotypes. Most Ad serotypes utilize the coxsackie-adenovirus-receptor (CAR) as a primary attachment receptor 1. This is, however, not the case for species B Ad serotypes. Recently, we have suggested a new grouping of species B Ads based on their

Contact: André Lieber, phone: (206) 221-3973, Fax: (206) 685-8675, lieber00@u.washington.edu.

Authors Contributions:

H.W. conducted the studies for the identification and validation of DSG2 as Ad receptor; Z.L. performed the immunofluorescence studies; Y.L performed the *in vivo* studies; J. P. contributed to adenovirus attachment assays; I. B. contributed to *in vivo* studies; T.H. helped with the expression array studies; D.K. and M.R.D. participated in *in vitro* studies with Herceptin; R.S. performed the Western blot studies for kinase activation; X.Z. produced the DSG2-expressing lentivirus vector; J.K.W. provided the DSG2-specific antibodies; N.U. and C.D. provided tumor biopsies; A.H. helped with data interpretation; P.F. performed the Biacore studies and provided recombinant PtDd, A.L. supervised the project and wrote the manuscript.

receptor usage 2. Group 1 (Ad16, 21, 35, 50) nearly exclusively utilize CD46 as a receptor; Group 2 (Ad3, Ad7, 14) share a common, unidentified receptor/s, which is not CD46 and which was tentatively named receptor X; Group 3 (Ad11) preferentially interacts with CD46, but also utilizes receptor X if CD46 is blocked.

Species B Ads are common human pathogens. Since 2005, a simultaneous emergence of diverse species B serotypes, including serotypes Ad3, Ad7, and Ad14, was observed. In 2007 a new, highly pathogenic and possibly more virulent strain of Ad14, Ad14a, has been discovered at several sites in the US and in Asia 3–4. We recently demonstrated that Ad14a belongs to species B group 2 Ads with regards to their receptor usage 5. Collectively, we will refer to all receptor X-utilizing serotypes (Ad3, Ad7, Ad14, Ad14a, Ad11) as AdB-2/3.

AdB-2/3 have potential as gene transfer vectors, particularly with regard to tumors of epithelial origin6. Epithelial cells maintain several intercellular junctions (tight junctions, adherens junctions, gap junctions, and desmosomes), a feature which is often conserved in epithelial cancers *in situ* and in cancer cell lines 7. Both CAR and CD46 are trapped in intercellular junctions of epithelial cancer cells and are not accessible to Ads that use these attachment receptors 8–9. In contrast, AdB-2/3 efficiently infect epithelial cancer cells, which is accomplished in part through induction of processes that are reminiscent of Epithelial-to-Mesenchymal Transition (EMT)8, a cellular transdifferentiation program where epithelial cells lose characteristics such as intercellular junctions and gain properties of mesenchymal cells 10. Another distinctive feature of AdB-2/3 is their ability to produce subviral dodecahedral particles during their replication, consisting of Ad fiber and penton base 11. Penton-Dodecahedra (PtDd) cannot assemble from full-length penton base protein, but require spontaneous N-terminal truncation by proteolysis between residues 37 and 38 12. This cleaved site is conserved in Ad3, Ad7, Ad11, and Ad14 but is not present in Ad2 and Ad5 (Supplementary Fig. 1a). In the case of Ad3, PtDd are formed at a massive excess (5.5×10^6 PtDd per infectious virus) and it has been hypothesized that PtDd contribute to virus escape and spreading 13.

The first attempts to identify receptor X date back to 1995. These initial studies indicated the interaction of Ad3 with a ~130 kDa HeLa cell protein 14. Recently, several candidates for receptor X such as CD46, CD80 and/or CD86 were suggested 15–18. However, we and others have thus far been unable to verify that these proteins can serve as the high affinity receptor for AdB-2/3 2,19–23.

In the present study, using Ad3 virions and recombinant Ad3 PtDd as a probe for receptor X, we identified desmoglein 2 (DSG2) as a high affinity receptor for AdB-2/3 serotypes. DSG2 is a calcium-binding transmembrane glycoprotein belonging to the cadherin protein family. In epithelial cells, DSG2 is a component of the cell-cell adhesion structure 24. Its cytoplasmic tail interacts with a series of proteins that are in direct contact with regulators of cell adhesion and intercellular junctions/ cell morphology 25. It has been shown that DSG2 is overexpressed in a series of epithelial malignancies including gastric cancer 26, squamous cell carcinomas 27, melanoma 28, metastatic prostate cancer 29, and bladder cancer 30.

Results

DSG2 is a receptor for AdB-2/3 viruses

Our previous studies showed that Ad3 binds at nanomolar affinity to a high-density cellular receptor 2. Ad3 binding was sensitive to trypsin and could be blocked by EDTA, implying that binding required divalent cations. First we sought to identify the Ad3 capsid protein that mediates high-affinity binding to cells, which we would later use to search for the high-affinity receptor X. Notably, high-affinity binding of Ad5 to CAR and Ad35 binding to CD46, respectively, is mediated by the corresponding fiber knob 31. Our previous studies, however, revealed that a recombinant, timeric Ad3 knob could not completely block Ad3 virus binding even when very high concentrations were used, indicating that other or additional capsid moieties are involved in Ad3 binding 32. Consequently, we utilized recombinant Ad3 dodecahedra composed of Ad3 penton bases (BsDd) or Ad3 penton bases and fibers (PtDd) (Supplementary Fig. 1b) 33 to compete for Ad3 binding. We showed that PtDd but not BsDd blocked attachment of Ad3 to cells (Fig. 1a). PtDd also blocked binding of other AdB-2/3, e.g. Ad14, Ad14a, as well as Ad11, if CD46 is also blocked. PtDd did, however, not inhibit binding of Ad5 and only partially blocked Ad35 binding (Fig. 1a, Supplementary Fig. 1c). Preincubation of cells with PtDd resulted in a better Ad3 binding inhibition than Ad3 knob mixed with BsDd (Supplementary Fig. 1d). The ability of PtDd to compete with Ad3 was also confirmed in transduction studies, where PtDd efficiently blocked an Ad3 vector (Ad3-GFP) but not the transduction of an Ad35 vector (Ad35-GFP (that uses CD46 as a receptor) (Fig. 1b). Ad3-GFP (Supplementary Fig. 1e) and Ad35-GFP 34 are wild-type Ad3- and Ad35-based vectors containing a CMV-GFP expression cassette inserted into the E3 region.

To select an optimal cell line for receptor X identification, we compared Ad3 virus binding to several human and animal cell lines (Fig. 1c). Ad3 did not bind to rodent cells suggesting that receptor X was not expressed or not accessible to Ad3 in these cells. Of the 10 human cell lines initially tested (HeLa, K562, SKOV3, 293, HT29, SKHep1, Saos, Y79, Ramos), Ad3 binding was absent only on Ramos (human Burkitt's lymphoma) cells.

To identify Ad receptor candidates, HeLa cell membrane proteins were solubilized, separated on polyacrylamide gels, and blotted. Blots were hybridized with viral particles and binding was visualized with virus fiber knob specific antibodies. Specific gel bands were excised and analyzed by tandem mass-spectroscopy (MS/MS). First, we tested whether this assay can detect a known Ad receptor, CD46. When filters were incubated with CD46-targeting Ad5/35++ virions35, a single band was found that matched CD46 (Fig. 1d). Incubation of filters with Ad3 virions revealed two bands with molecular weights of 160 kDa and 90 kDa (Fig. 1e). In addition to these two bands, Ad3 PtDd also reacted with HeLa proteins in the range of 130 kDa. Both 160 and 90 kDa bands were absent in Ramos cells, i.e. cells that do not bind Ad3. The ~130 kDa PtDd-binding band appeared in both HeLa and Ramos cells suggesting that it is not an Ad3 virus receptor. MS/MS-analysis of the 160 kDa band identified 14 peptides matching human desmoglein 2 (DSG2) (Fig. 1f). IP/Western analyses of HeLa membrane proteins demonstrated that both the 160 and 90 kDa bands were recognized by DSG2-specific antibodies (Fig. 1e, right panel). This is in aggreement with

previous Western blot studies showing that the 160 kDa band represents full size DSG2, and that the 90 kDa band is a DSG2 variant that lacks the intracellular domain, the transmembrane domain, and the juxtamembrane extracellular anchor domain 36–37.

BIAcore surface plasmon resonance (SPR) studies with sensors containing immobilized recombinant human DSG2 demonstrated that Ad3, but not Ad2 or Ad5, virions interact with DSG2 (Fig. 1g). Recombinant PtDd but not BsDd particles bound to DSG2 (Fig. 1h). The K_D (equilibrium dissociation constant) of PtDd –DSG2 interaction was 2.5 nM. PtDd binding to immobilized DSG2 was specific as soluble DSG2 competed with it (Supplementary Fig. 2). SPR analysis of binding kinetics also showed that Ad3 fiber knob dissociates faster from DSG2, which suggests the existence of additional DSG2 binding site(s) within the fiber shaft and/or the requirement of fiber multimerization for high affinity binding to DSG2 (Fig.1 i, also see Supplementary Fig. 1d).

Loss- and gain-of-function studies were performed on cell lines to validate DSG2 as a critical receptor for AdB-2/3 binding/infection. Recombinant DSG2 protein blocked the binding of Ad3 as well as other AdB2/3 Ads, i.e. Ad7, Ad14, Ad14a, and Ad11 to HeLa cells, but not the binding of Ad5 and Ad35 (Fig. 2a). Ad3-GFP infection was efficiently inhibited by DSG2 protein but not by other structurally related members of the cadherin superfamily (desmoglein 1-DSG1 and desmocollin 1-DSC1) 38 (Fig. 2b). This study also showed that DSG2 protein had no effect on transduction by the CD46-targeting vector (Ad35-GFP). Significant inhibition of Ad3 attachment was observed with monoclonal antibodies (mAbs) against extracellular domains 3 and 4 (Fig. 2c) (for a scheme of DSG2, see Fig. 1f). Transfection of HeLa cells with a pool of *DSG2*-specific siRNAs resulted in ~7-fold downregulation of surface DSG2 levels (Supplementary Fig. 3a). Ad3 attachment was 3 fold lower in *DSG2*-siRNA treated HeLa cells compared to control siRNA-treated cells ($p<0.001$) (Fig. 2d). GFP expression levels after infection with Ad3-GFP were 13.9-fold lower in *DSG2*-siRNA transfected cells than in control siRNA transfected cells (Fig. 2e). *DSG2*-specific siRNA did not affect transduction with the CAR-targeting vector Ad5-GFP. However, *DSG2*-siRNA transfection also decreased binding and transduction with the CD46-specific vectors Ad35-GFP and Ad5/35-GFP. *DSG2*-siRNA did not decrease CD46 levels in HeLa cells. At this point we cannot explain this phenomenon. It appears, however, to be specific to HeLa cells. No decrease in Ad35-GFP or Ad5/35-GFP transduction was detected in 293 cells (Supplementary Figs. 3b–d) or breast cancer BT474 cells that were transfected with *DSG2*-siRNA.

siRNA mediated DSG2 downregulation also decreased viral cytolysis and spread in cells that were infected at 100% confluence at an MOI of one Ad3-GFP pfu per cell. Using adjusted MOIs (to achieve comparable percentages of GFP expression at 16 hours post-infection), we followed viral cytolysis over time and found larger lytic plaques in control siRNA than in *DSG2* siRNA-transfected cells at day 7 p.i. This is reflected in crystal violet staining of viable cells that remained attached to tissue culture wells, i.e. cells that did not develop cytopathic effects due to virus infection (Fig. 2f). Quantitative analysis of cell viability showed significantly less cell killing in cells in which DSG2 was downregulated by siRNA compared to control siRNA treated cells (Fig. 2g).

For gain-of-function studies, we selected a series of cell lines with different DSG2 expression levels and measured Ad3-GFP transduction (Fig.3a and Supplementary Figs. 3e–g). All cell lines that lacked DSG2 expression (lymphoma Ramos, Raji, Mino, and HH cells) were refractory to Ad3-GFP transduction but could be transduced by the CD46 targeting Ad5/35-GFP vector (because CD46 is expressed on these cells 39). DSG2-positive K562 cells, on the other hand, could be efficiently transduced with Ad3-GFP. About 70% of BJAB cells were DSG2 positive and, correspondingly, the percentage of GFP-positive cells reached a plateau at about 50%. To conclusively prove the critical role of DSG2 in Ad3 infection, we ectopically expressed DSG2 via lentivirus vector gene transfer in the histiocytic lymphoma cell line U937, which is refractory to Ad3-GFP transduction (Fig. 3b). Ectopic DSG2 expression in U937-DSG2 cells conferred efficient Ad3 attachment and transduction, whereas Ad35 attachment and Ad5/35-GFP transduction was unaffected in these cells (Figs. 3c and d).

DSG2 localization in human cells

As expected, we found DSG2 in cell membranes of normal epithelial tissues (foreskin and colon) and epithelial cancers (breast and ovarian cancer) (Fig. 4a). Confocal immunofluorescence microscopy studies of polarized colon cancer T84 and CaCo-2 cells demonstrated colocalization of DSG2 and the intercellular junction protein Claudin 7 (Fig. 4b and Supplementary Figs. 4a and b). In stacked XZ image sections (Fig. 4b) {or XY sections taken at different depth of the cell layer (Supplementary Fig. 4a)}, DSG2 appears at the distal end of intercellular junctions. DSG2 also colocalized with the adherens junction protein E-cadherin in epithelial cells (Supplementary Figs. 4c and d).Fifteen minutes after adding Cy3-labelled Ad3 to polarized cells, viral particles were detectable in association with junction-localized DSG2 (Fig. 4c and Supplementary Fig.4b, lower right panel). Similar results were obtained with normal small airway epithelial cells incubated with PtDd for 15 min as shown by triple labeling of Cy5-PtDd, DSG2, and E-cadherin (Fig. 4d, upper panel). PtDd signals were on cell membranes (Fig. 4d, lower panel, thin arrows) and in the cytoplasm (thick arrows), most likely reflecting internalized particles (see also Supplementary Fig. 4e).

In contrast to polarized epithelial cell lines, in non-polarized cells, such as HeLa cells, intercellular junctions (i.e. membrane-localized Claudin 7 and E-cadherin signals) were absent. DSG2 and Ad3 were found dispersed over the cell surface (Fig. 4e).

Our studies on Ad3 infection of HeLa cells (Figs. 1 and 2) indicate that DSG2 also acts as receptor in non-polarized cells. In this context, it is noteworthy that we detected DSG2 and Ad3 binding/transduction in human platelets and granulocytes (Supplementary Figs. 5a and b). Although these findings are relevant for Ad3 pathogenesis and the intravascular application of Ad3 vectors for gene therapy purposes, we focused in this study on analyzing the consequences of Ad3-DSG2 interaction in polarized epithelial cells.

Ad3 interaction with DSG2 triggers EMT

Recently, we found that AdB-2/3 interaction with epithelial ovarian cancer cells triggered EMT. EMT is characterized by increased expression of mesenchymal markers, increased

expression of extracellular matrix compounds, decreased expression of epithelial markers, altered location of transcription factors, and activation of kinases 7. Here, we attempted to prove that Ad3 interaction with DSG2 triggers EMT-like events. To avoid potential side effects of viral gene expression on cell morphology, the studies utilized ultraviolet light (UV)-inactivated Ad particles and recombinant Ad3 PtDd. Overall, the results with both types of particles were similar. Incubation of epithelial cancer cells with PtDd (Fig. 5) or UV-inactivated Ad3 (not shown) caused remodeling of junctions as reflected by the decrease in of membrane/junction-localized Claudin 7 (Fig. 5a) or E-cadherin signals (Fig. 5b). Furthermore, after PtDd treatment we found stronger immunofluorescence signals of the mesenchymal markers Vimentin and Lipocalin 2 (Figs. 5c and d). To identify intracellular signaling pathways triggered by PtDd interaction with DSG2, we studied mRNA expression profiles. Twelve hours after incubation of polarized BT474 cells with PBS, BsDd, or PtDd, mRNA was analyzed using Affymetrix human ST gene arrays. We found that PtDd treatment resulted in >1.5-fold upregulation of 430 genes and >1.5-fold down-regulation of 352 genes when compared to PBS-treated cells (Fig. 5e). The list of altered genes was further processed by Pathway-Express software 40. This computation suggested that PtDd mediated marked activation of a number of signaling pathways involved in EMT, including phosphatidylinositol (PI), mitogen activated protein kinase (MAPK aka ERK), Wnt, adherens junctions, focal adhesion, and regulation of actin cytoskeleton signaling pathways (Supplementary Fig. 6).

Western blot analysis using phosphorylation-specific antibodies showed that PtDd, but not BsDd, triggered the activation of PI3K and MAPK/ERK1/2, i.e. key kinases involved in EMT (Fig. 5f). Activation of these pathways was also triggered by DSG2-specific mAbs (6D8, and to a lesser degree 10D2, and 13B11) but not with mAbs directed against CD46. PtDd activation of pathways was mediated by DSG2, because MAPK/ERK1/2 and PI3K phosphorylation was decreased in cells transfected with *DSG2* siRNA but not in control siRNA treated cells. Finally, PtDd-triggered phosphorylation of kinases was absent when cells were pretreated with the ERK1/2 inhibitor UO126 (upper panel) or the PI3K inhibitor Wortmannin (lower panel). Taken together, our data suggest that Ad3 or Ad3PtDd binding to DSG2 triggers EMT in epithelial cells.

Ad3 and PtDd increase access to receptors that are trapped in intercellular junctions

To test whether Ad3 virion- or Ad3 PtDd-triggered EMT also results in opening of intercellular junctions, we studied barrier properties in monolayer of epithelial cells. First we measured the flux of 4 kDa FITC-dextran through confluent polarized BT474 cells cultured in transwell chambers (Fig. 6a). We found that PtDd but not BsDd incubation significantly increased the permeability coefficient compared to PBS. We then tested whether Ad3 or PtDd-triggered EMT and transient junction-opening would increase access to proteins that are normally not accessible due to epithelial cell junctions. An example for such a junction-localized receptor is CD46, the high-affinity receptor for Ad35 and Ad5/35 8. We confirmed that a large number of CD46 molecules localizes to junctions of BT474 cells (Fig. 6b, left panels). PtDd pre-treatment significantly increased the attachment of ^{3}H-Ad35 to BT474 cells when compared to BsDd treatment (Fig. 6b, right panel). An enhancing effect of PtDd on transduction of CD46-targeting Ad vectors was also demonstrated *in vivo* in

subcutaneous epithelial tumors (Fig. 6c). Intravenous injection of PtDd eight hours before application of Ad5/35-bGal increased viral transduction. Beta-galactosidase activity, measured in tumor lysates 3 days after Ad injection, was 2.3(+/−0.2)× 10^5 rlu/μg protein, 2.7(+/−0.6)× 10^5 rlu/μg, and 38(+/−3.5)× 10^5 rlu/μg for mice that were mock-injected, BsDd-coinjected, and PtDd-coinjected, respectively.

In another line of experiments in breast cancer cell cultures, we found that Her2/*neu*, the receptor for the widely used monoclonal antibody Herceptin (trastuzumab) co-stained with the intercellular junction protein Claudin 7 (Fig. 6d). This suggests that not all Her2/*neu* molecules are accessible to Herceptin. Incubation of the Her2/*neu*-positive breast cancer cell line BT474 with PtDd triggered relocalization of Her2/*neu* to the cell surface (Fig. 6e). To consolidate this obersvation, we tested whether Ad3 or Ad3PtDd would improve BT474 cell killing by Herceptin. In agreement with earlier studies 41, Herceptin caused death of approximately 25% of BT474 cells cells (Fig. 6f). Pre-incubation of BT474 cells with UV-inactivated Ad3 particles or PtDd increased Herceptin cytotoxicity by more than 2-fold. Incubation with UV-inactivated Ad5 particles or BsDd had no effect on Herceptin killing. In addition, Herceptin and PtDd/Herceptin had no cytotoxic effect on the Her2/*neu*-negative breast cancer cell line MDA-MB-231 (Supplementary Fig. 7a). The enhancing effect of PtDd and Ad3 on Herceptin killing of BT474 cells was mediated by DSG2, as downregulation of DSG2 in BT474 cells by *DSG2* siRNA abolished this effect (Fig. 6g). We also studied whether inhibition of key pathways involved in EMT affects the enhancing effect of PtDd on Herceptin cytotoxicity. These studies showed that inhibtion of PI3K by Wortmannin, as well as inhibition of MAPK/ERK by UO126 counteracted PtDd enhancement of Herceptin therapy (Fig. 6g). Importantly, intravenous injection of PtDd (2 mg/kg) into BT474-M1-tumor-bearing mice before Herceptin treatment resulted in elimination of tumors, an outcome that could not be achieved with Herceptin injection alone (Fig. 6h). PtDd pretreatment also allowed the unfolding of the therapeutic effect of the EGFR-specific mAb Erbitux (cetuximab) as it increased killing of EGFR-positive colon cancer LoVo cells with this antibody *in vitro* (Supplementary Fig. 7b).

Discussion

In this study we describe two major findings: *i)* DSG2 is a receptor crucial for infection of a series of human adenoviruses that are common pathogens and important biomedical tools. *ii)* Ad interaction with DSG2 results in the opening of intercellular junctions, thus increasing access to receptors trapped therein.

DSG2 is an Ad attachment receptor

The use of complete Ad3 particles or PtDd as a receptor probe was instrumental in the identification of DSG2 as the attachment receptor for Ad3, Ad7, Ad11, and Ad14. Previous attempts with Ad3 fiber knob domains as a bait did not yield meaningful receptor candidates 32. Our competition and surface plasmon resonance studies shown in Figure 1, indicate that the DSG2 interacting domain(s) within Ad3 are formed by the fiber only in the spatial constellation that is present in viral particles. This clearly widens our understanding of Ad

attachment echanisms, which, so far, were thought to involve only a high affinity interaction between the fiber knob and the cellular receptor, i.e. CAR or CD46.

Role of Ad3 and PtDd interaction with DSG2 in viral dissemination

During replication of Ad5, excess production of fiber results in the disruption of epithelial junctions either by interfering with CAR dimerization (which is critical for maintenance of junctions) or by triggering intracellular signaling that leads to reorganization of intercellular junctions 42–43. Both mechanisms could also be involved in Ad3 virion/DSG2- and Ad3 PtDd/DSG2-mediated intercellular junction opening. We have experimental support for intracellular signaling triggered by Ad3 and PtDd binding to DSG2 in epithelial cells. Immunofluorescence, PI3K/MAPK phosphorylation, mRNA expression array, and metabolic pathway inhibition data suggest that Ad3 and PtDd trigger EMT in epithelial cells resulting in transient opening of intercellular junctions. Intercellular junction opening mediated by interaction of Ad3 particles or recombinant PtDd with DSG2 is further supported by increased cell permeability and access to receptors that are trapped in intercellular junctions (CD46 and Her2/*neu*). Along this line, a recent study showed that antibodies against the extracellular domain of DSG2 resulted in the opening of intercellular junctions in CaCo-2 cell monolayers 44.

Ad3 virion- and PtDd-triggered EMT, i.e. the dissociation of the intercellular junctions, appears to have an important biological role. We speculate that, specifically the massive overproduction of PtDd during viral infection and its interaction with DSG2, facilitate the lateral viral spread in epithelial cells and, potentially, the penetration of Ad into subepithelial cell layers and the blood stream.

Implications for Ad pathogenesis

Our findings that DSG2 is an attachment receptor that facilitates further viral spread, sheds light on the Ad3 infection mechanism of the respiratory tract epithelium. Furthermore, the observation that Ad3 binds to DSG2 on platelet and granulocytes has potential implications on systemic spread of this virus once it has entered the blood stream. Although mouse DSG2 shares 76% homology with human DSG2 45, our data, showing that mouse cells are refractory to Ad3-GFP infection, indicate that mouse DSG2 cannot function as an Ad3 receptor. To study pathogenesis of AdB-2/3 serotypes, transgenic mice that express human DSG2 under the control of adequate endogenous regulatory elements resulting in DSG2 expression in a pattern and at levels similar to humans, would be a critical tool.

Implications for cancer therapy

DSG2 has been proposed as a marker for epithelial tumors 46. The epithelial phenotype of cancer cells and the ability to form physical barriers represent a mechanism that restricts access of drugs, antibodies, oncolytic viruses, or immune cells to the sites of tumors, thus diminishing the efficacy of such therapeutic modalities 47. We demonstrated here, in three examples (Ad5/35 vectors, Herceptin, and Erbitux), that this important problem in cancer therapy can perhaps be addressed by the use of DSG2-interacting Ad3 components. While our initial data with PtDd are promising, studies in appropriate *DSG2* transgenic mouse models are required to gain further preclinical safety information for this approach.

In conclusion, we report the discovery of the high affinity receptor for a series of common human Ads. Our study contributes to the understanding of how Ads induce cellular processes in order to gain access to epithelial tissue. Our findings have implications for improving cancer therapies.

Gene array data has been deposited at NCBI Gene Expression Omnibus (http://www.ncbi.nlm.nih.gov/geo) under accession number GSE24138.

Methods

Proteins and antibodies

The knob domains of Ad3, Ad5, and Ad35 fibers were produced in E.coli as described elsewhere 48. Recombinant Ad3 penton-dodecahedra (PtDd) and base dodecahedra (BsDd) were produced in insect cells and purified as described previously 33. A complete list of antibodies can be found in the SI. Polyclonal rabbit antibodies against purified recombinant Ad3 and Ad35K++ knob were produced by PickCell Laboratories B.V. (Amsterdam, The Netherlands). DSG2-specific monoclonal antibodies 20G1, 7H9, 13B11, 10D2 and 8E5 49 were purified from hybridoma culture supernatant.

Cell lines

Cells were cultured as described in the SI. BT474 is a Her2/*neu*-positive breast cancer cell line with epithelial cell features. To achieve cell polarization, 1.4×10^5 BT474, T84 and CaCo-2 cells were cultured in collagen-coated 6.5 mm Transwell inserts (0.4μm pore size) (Costar Transwell Clears) for 10 days until transepithelial resistance was stable.

Adenoviruses

Wild-typeAd3 (GB strain), Ad7p (Gomen stain), Ad11p (Slobitski strain), Ad14 (DeWit strain), and Ad35 (Holden strain) were obtained from the ATCC. Ad14a is new genomic variant of Ad14 5. Propagation, methyl-^{3}H thymidine labeling, purification and titering of Ads was performed as described elsewhere 2. Ad5/35-GFP and Ad5-GFP are Ad5 vectors containing Ad35 and Ad5 fibers and a CMV-GFP expression cassette 50. Ad3-GFP and Ad35-GFP are wild-type Ad3- and Ad35-based vectors containing a CMV-GFP expression cassette inserted into the E3 region. Construction of Ad3-GFP is described in SI. Ad35-GFP has been described previously 34. For transduction studies, cells were exposed to Ad vectors at the indicated MOIs for one hour, washed, and GFP expression was measured by flow cytometry 18 hours later.

Membrane protein preparation

HeLa cell membrane proteins were prepared as described earlier 51. Briefly, HeLa cell pellets were re-suspended in ice-cold homogenization buffer (20 mM Hepes, 1.5 mM $MgCl_2$, 5 mM KCl, 150 mM NaCl, 15% glycerol, 0.25 M sucrose, 0.1 mM EDTA, 2 mM β-mercaptoethanol, 1 mM PMSF). After disruption with a 3 ml syringe and 21G needle, the lysate was centrifuged at 400 × g for 15 minutes. The supernatant was diluted with 2 times volume of PBS and centrifuged at 35,000 rpm for 1 hour in a Beckman ultracentrifuge. The membrane protein pellet was resuspended in solubilization buffer (50 mM Hepes, 5 mM

$MgCl_2$, 5 mM KCl, 150 mM NaCl, 15% glycerol, 0.25 M sucrose, 0.1 mM EDTA, 2 mM β-mercaptoethanol, 1 mM PMSF, 0.5% Brij 96V(Fluka, St Louis, MO). The use of Brij96V as a detergent was intrumental as desmosomal proteins are highly insoluble.

Western blot with Ad3 and PtDd

Technical details for mass-spectroscopy analysis are described elsewhere 51. To immunoprecipitate DSG2 from soluble crude membrane protein preparations, DSG2-specific mAb 6D8, and the Pierce Crosslink Immunoprecipitation Kit (Pierce Biotechnology, Rockford, IL) were used. Crude membrane proteins from HeLa cells were solubilized with 0.5% detergent Brij 96V, pre-incubated with control resin for 3 hours at 4°C to reduce unspecific binding, and then incubated with DSG2 antibody crosslinked proteinA/G agarose overnight at 4°C. Bound protein were eluted per manufacturer's instruction.

Surface plasmon resonance (SPR) analyses

Acquisitions were done on a BIAcore 3000 instrument. HBS-N (GE-Healthcare, Pittsburgh, PA) supplemented with 2 mM $CaCl_2$ was used as running buffer in all experiments at a flowrate of 5 μl min^{-1}. Immobilisation on CM4 sensorchip (BIAcore) was performed using DSG2 (Leinco Technology, Inc) at 0.1 mg ml^{-1} diluted in 10 mM sodium acetate buffer pH4.2 injected for 10 minutes on EDC-NHS activated flow-cell. A control flow-cell was activated by EDC-NHS and inactivated by ethanolamine. Different concentration of PtDd, BsDd, Ad3 fiber knob were injected for 5 minutes followed by 3 minutes dissociation time and the signal was automatically subtracted from the background of the ethanolamine deactivated EDC-NHS flow cell. For the adenovirus binding experiments, a similar protocol was used with the injection of wild-type Ad2, Ad3 and Ad5 at 5.10^9 vp per ml.

siRNA studies

A set of *DSG2* specific siRNA was synthesized by Dharmacon (Thermo Scientific). The target sequences were CAAUAUACCUGUAGUAGAA, GAGAGGAUCUGUCCAAGAA, CCUUAGAGCUACGCAUUAA and CCAGUGUUCUACCUAAAUA. Control siRNA was purchased from Qiagen, Valencia, CA. siRNA transfection was performed using HyperFect transfection reagent (Qiagen).

DSG2 expressing U937 cells

DSG2 cDNA (accession No. BC099657) from Capital Biosciences (Rockville, MD) was cloned into the lentivirus vector pRRL-SIN 52 under the control of the EF1α promoter. VSVG-pseudotyped lentivirus vectors was produced and titered as described earlier 53.

Animal studies

All experiments involving animals were conducted in accordance with the institutional guidelines set forth by the University of Washington. Mice were housed in specific-pathogen-free facilities. Breast cancer xenografts were established by injecting cancer cells in matrigel (1:1 vol/vol) into the mammary fat pad of CB17 SCID-beige mice. Herceptin

was injected intraperitoneally at a dose of 10 mg/kg. PtDd was given intravenously at a dose of 2 mg/kg. Tumor volumes were measured as described previously54.

Supplementary Material

Refer to Web version on PubMed Central for supplementary material.

Acknowledgments

The work was supported by NIH grants R01 CA080192, R01 HLA078836, and Pacific Ovarian Cancer Research Consortium/Specialized Program of Research Excellence in Ovarian Cancer Grant P50 CA83636. We thank Ruan van Rensburg for critical comments and the Functional Genomics Core at Center for Ecogenetics and Environmental Health, School of Public Health University of Washington for array analysis.

References

1. Bergelson JM, et al. Isolation of a common receptor for Coxsackie B viruses and adenoviruses 2 and 5. Science. 1997; 275:1320–1323. [PubMed: 9036860]
2. Tuve S, et al. A new group B adenovirus receptor is expressed at high levels on human stem and tumor cells. J Virol. 2006; 80:12109–12120. [PubMed: 17020944]
3. Louie JK, et al. Severe pneumonia due to adenovirus serotype 14: a new respiratory threat? Clin Infect Dis. 2008; 46:421–425. [PubMed: 18173356]
4. Tate JE, et al. Outbreak of severe respiratory disease associated with emergent human adenovirus serotype 14 at a US air force training facility in 2007. J Infect Dis. 2009; 199:1419–1426. [PubMed: 19351260]
5. Wang H, Tuve S, Erdman DD, Lieber A. Receptor usage of a newly emergent adenovirus type 14. Virology. 2009; 387:436–441. [PubMed: 19307010]
6. Yamamoto M, Curiel DT. Current issues and future directions of oncolytic adenoviruses. Mol Ther. 2010; 18:243–250. [PubMed: 19935777]
7. Turley EA, Veiseh M, Radisky DC, Bissell MJ. Mechanisms of Disease: epithelial-mesenchymal transition-does cellular plasticity fuel neoplastic progression? Nat Clin Pract Oncol. 2008
8. Strauss R, et al. Epithelial phenotype of ovarian cancer mediates resistance to oncolytic adenoviruses. Cancer Research. 2009; 15:5115–5125. [PubMed: 19491256]
9. Coyne CB, Bergelson JM. CAR: a virus receptor within the tight junction. Adv Drug Deliv Rev. 2005; 57:869–882. [PubMed: 15820557]
10. Thiery JP, Sleeman JP. Complex networks orchestrate epithelial-mesenchymal transitions. Nat Rev Mol Cell Biol. 2006; 7:131–142. [PubMed: 16493418]
11. Norrby E, Nyberg B, Skaaret P, Lengyel A. Separation and characterization of soluble adenovirus type 9 components. J Virol. 1967; 1:1101–1108. [PubMed: 5630229]
12. Fuschiotti P, et al. Structure of the dodecahedral penton particle from human adenovirus type 3. J Mol Biol. 2006; 356:510–520. [PubMed: 16375921]
13. Fender P, Boussaid A, Mezin P, Chroboczek J. Synthesis, cellular localization, and quantification of penton-dodecahedron in serotype 3 adenovirus-infected cells. Virology. 2005; 340:167–173. [PubMed: 16040074]
14. Di Guilmi AM, Barge A, Kitts P, Gout E, Chroboczek J. Human adenovirus serotype 3 (Ad3) and the Ad3 fiber protein bind to a 130-kDa membrane protein on HeLa cells. Virus Res. 1995; 38:71–81. [PubMed: 8546011]
15. Fleischli C, et al. Species B adenovirus serotypes 3, 7, 11 and 35 share similar binding sites on the membrane cofactor protein CD46 receptor. J Gen Virol. 2007; 88:2925–2934. [PubMed: 17947513]
16. Short JJ, et al. Adenovirus serotype 3 utilizes CD80 (B7.1) and CD86 (B7.2) as cellular attachment receptors. Virology. 2004; 322:349–359. [PubMed: 15110532]

17. Short JJ, Vasu C, Holterman MJ, Curiel DT, Pereboev A. Members of adenovirus species B utilize CD80 and CD86 as cellular attachment receptors. Virus Res. 2006; 122:144–153. [PubMed: 16920215]
18. Sirena D, et al. The human membrane cofactor CD46 is a receptor for species B adenovirus serotype 3. J Virol. 2004; 78:4454–4462. [PubMed: 15078926]
19. Gaggar A, Shayakhmetov DM, Lieber A. CD46 is a cellular receptor for group B adenoviruses. Nat Med. 2003; 9:1408–1412. [PubMed: 14566335]
20. Marttila M, et al. CD46 is a cellular receptor for all species B adenoviruses except types 3 and 7. J Virol. 2005; 79:14429–14436. [PubMed: 16254377]
21. Segerman A, Arnberg N, Erikson A, Lindman K, Wadell G. There are two different species B adenovirus receptors: sBAR, common to species B1 and B2 adenoviruses, and sB2AR, exclusively used by species B2 adenoviruses. J Virol. 2003; 77:1157–1162. [PubMed: 12502832]
22. Gustafsson DJ, Segerman A, Lindman K, Mei YF, Wadell G. The Arg279Gln [corrected] substitution in the adenovirus type 11p (Ad11p) fiber knob abolishes EDTA-resistant binding to A549 and CHO-CD46 cells, converting the phenotype to that of Ad7p. J Virol. 2006; 80:1897–1905. [PubMed: 16439545]
23. Persson BD, et al. An arginine switch in the species B adenovirus knob determines high-affinity engagement of the cellular receptor CD46. J Virol. 2008
24. Chitaev NA, Troyanovsky SM. Direct Ca2+-dependent heterophilic interaction between desmosomal cadherins, desmoglein and desmocollin, contributes to cell-cell adhesion. J Cell Biol. 1997; 138:193–201. [PubMed: 9214392]
25. Cowin P. Unraveling the cytoplasmic interactions of the cadherin superfamily. Proc Natl Acad Sci U S A. 1994; 91:10759–10761. [PubMed: 7971957]
26. Biedermann K, et al. Desmoglein 2 is expressed abnormally rather than mutated in familial and sporadic gastric cancer. J Pathol. 2005; 207:199–206. [PubMed: 16025435]
27. Harada H, Iwatsuki K, Ohtsuka M, Han GW, Kaneko F. Abnormal desmoglein expression by squamous cell carcinoma cells. Acta Derm Venereol. 1996; 76:417–420. [PubMed: 8982400]
28. Schmitt CJ, et al. Homo- and heterotypic cell contacts in malignant melanoma cells and desmoglein 2 as a novel solitary surface glycoprotein. J Invest Dermatol. 2007; 127:2191–2206. [PubMed: 17495963]
29. Trojan L, et al. Identification of metastasis-associated genes in prostate cancer by genetic profiling of human prostate cancer cell lines. Anticancer Res. 2005; 25:183–191. [PubMed: 15816537]
30. Abbod MF, Hamdy FC, Linkens DA, Catto JW. Predictive modeling in cancer: where systems biology meets the stock market. Expert Rev Anticancer Ther. 2009; 9:867–870. [PubMed: 19589024]
31. Leopold PL, Crystal RG. Intracellular trafficking of adenovirus: many means to many ends. Adv Drug Deliv Rev. 2007; 59:810–821. [PubMed: 17707546]
32. Tuve S, et al. Role of cellular heparan sulfate proteoglycans in infection of human adenovirus serotype 3 and 35. PLoS Pathog. 2008; 4:e1000189. [PubMed: 18974862]
33. Fender P, Ruigrok RW, Gout E, Buffet S, Chroboczek J. Adenovirus dodecahedron, a new vector for human gene transfer. Nat Biotechnol. 1997; 15:52–56. [PubMed: 9035106]
34. Gao W, Robbins PD, Gambotto A. Human adenovirus type 35: nucleotide sequence and vector development. Gene Ther. 2003; 10:1941–1949. [PubMed: 14528318]
35. Wang H, et al. In vitro and in vivo properties of adenovirus vectors with increased affinity to CD46. J Virol. 2008; 82:10567–10579. [PubMed: 18753195]
36. Nava P, et al. Desmoglein-2: a novel regulator of apoptosis in the intestinal epithelium. Mol Biol Cell. 2007; 18:4565–4578. [PubMed: 17804817]
37. Kowalczyk AP, et al. Structure and function of desmosomal transmembrane core and plaque molecules. Biophys Chem. 1994; 50:97–112. [PubMed: 8011944]
38. Getsios S, Huen AC, Green KJ. Working out the strength and flexibility of desmosomes. Nat Rev Mol Cell Biol. 2004; 5:271–281. [PubMed: 15071552]
39. Wang H, et al. A recombinant adenovirus type 35 fiber knob protein sensitizes lymphoma cells to rituximab therapy. Blood. 2010; 115:592–600. [PubMed: 19965652]

40. Khatri P, et al. New Onto-Tools: Promoter-Express, nsSNPCounter and Onto-Translate. Nucleic Acids Res. 2006; 34:W626–W631. [PubMed: 16845086]
41. Bostrom J, et al. Variants of the antibody herceptin that interact with HER2 and VEGF at the antigen binding site. Science. 2009; 323:1610–1614. [PubMed: 19299620]
42. Walters RW, et al. Adenovirus fiber disrupts CAR-mediated intercellular adhesion allowing virus escape. Cell. 2002; 110:789–799. [PubMed: 12297051]
43. Coyne CB, Shen L, Turner JR, Bergelson JM. Coxsackievirus entry across epithelial tight junctions requires occludin and the small GTPases Rab34 and Rab5. Cell Host Microbe. 2007; 2:181–192. [PubMed: 18005733]
44. Schlegel N, et al. Desmoglein 2-mediated adhesion is required for intestinal epithelial barrier integrity. Am J Physiol Gastrointest Liver Physiol. 2010; 298:G774–G783. [PubMed: 20224006]
45. Mahoney MG, Simpson A, Aho S, Uitto J, Pulkkinen L. Interspecies conservation and differential expression of mouse desmoglein gene family. Exp Dermatol. 2002; 11:115–125. [PubMed: 11994138]
46. Schafer S, Koch PJ, Franke WW. Identification of the ubiquitous human desmoglein, Dsg2, and the expression catalogue of the desmoglein subfamily of desmosomal cadherins. Exp Cell Res. 1994; 211:391–399. [PubMed: 8143788]
47. Green SK, Karlsson MC, Ravetch JV, Kerbel RS. Disruption of cell-cell adhesion enhances antibody-dependent cellular cytotoxicity: implications for antibody-based therapeutics of cancer. Cancer Res. 2002; 62:6891–6900. [PubMed: 12460904]
48. Wang H, et al. Identification of CD46 binding sites within the adenovirus serotype 35 fiber knob. J Virol. 2007; 81:12785–12792. [PubMed: 17898059]
49. Keim SA, Johnson KR, Wheelock MJ, Wahl JK 3rd. Generation and characterization of monoclonal antibodies against the proregion of human desmoglein-2. Hybridoma (Larchmt). 2008; 27:249–258. [PubMed: 18707543]
50. Shayakhmetov DM, Papayannopoulou T, Stamatoyannopoulos G, Lieber A. Efficient gene transfer into human CD34(+) cells by a retargeted adenovirus vector. J Virol. 2000; 74:2567–2583. [PubMed: 10684271]
51. Gaggar A, Shayakhmetov D, Lieber A. Identifying functional adenovirus-host interactions using tandem mass spectrometry. Methods Mol Med. 2007; 131:141–155. [PubMed: 17656781]
52. Seppen J, Barry SC, Harder B, Osborne WR. Lentivirus administration to rat muscle provides efficient sustained expression of erythropoietin. Blood. 2001; 98:594–596. [PubMed: 11468155]
53. Li Z, et al. Toward a stem cell gene therapy for breast cancer. Blood. 2009; 113:5423–5433. [PubMed: 19329780]
54. Tuve S, et al. Combination of tumor site-located CTL-associated antigen-4 blockade and systemic regulatory T-cell depletion induces tumor-destructive immune responses. Cancer Res. 2007; 67:5929–5939. [PubMed: 17575163]

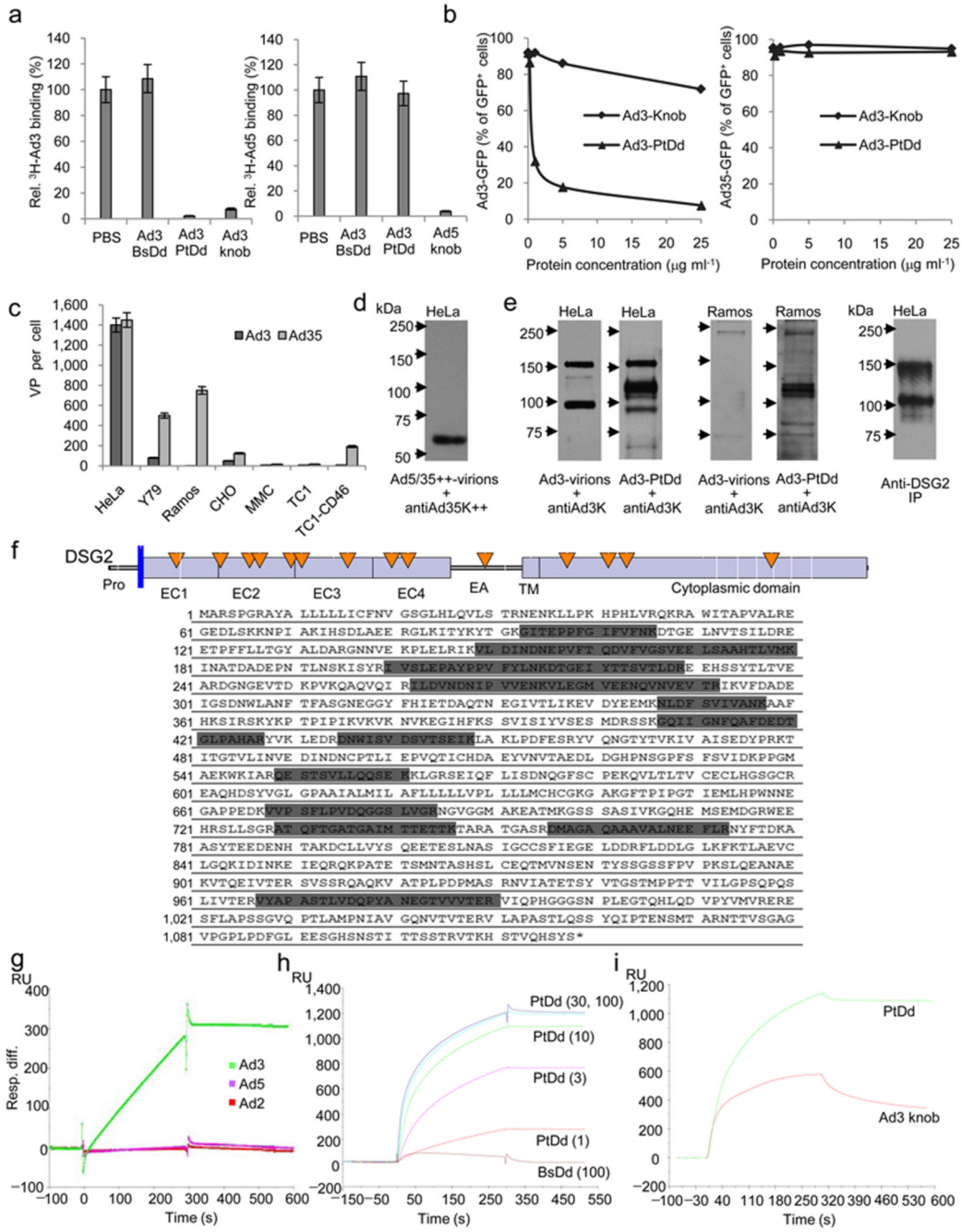

Fig.1. Identification of receptor X using Ad3 virions and Ad3 PtDd

a) Competition of ^{3}H-labeled Ad3 and Ad5 virus attachment to HeLa cells after pre-incubation with Ad3 BsDd, PtDd, or Ad fiber knobs. Attachment in PBS-treated cells was taken as 100%. N=5. Data are represented as mean +/− SEM). Ad3-PtDd vs. Ad3 knob: p=0.0033. **b)** Competition of Ad3-GFP and Ad35-GFP virus infection. HeLa cells were pretreated with Ad3 fiber knob or PtDd at increasing concentrations and then exposed to Ad3-GFP (left panel) or Ad35-GFP virus (right panel) at an MOI of 100pfu/cell. GFP expression was measured 18 hours later by flow cytometry. Data are represented as mean.

Standard deviation was less than 10% for all data points. **c)** Attachment of ^{3}H-labeled Ad3 and Ad35 viruses to human and non-human cell lines. Y79 and Ramos are human retinoblastoma and lymphoma cells, respectively. CHO cells are Chinese Hamster ovary cells. MMC and TC1 cells are mouse mammary carcinoma and lung carcinoma cells, respectively. TC1-CD46 cells express human CD46. Shown are the average number of viral particels attached per cells. N=5. **d and e)** Identification of receptor X by affinity capture and MS/MS. Membrane protein fractions were prepared from HeLa and Ramos cells. Protein blots were hybridized with Ad5/35++ virions (d) and Ad3 virions or Ad3 PtDd (e). Binding was visualized with polyclonal antibodies against Ad35++ knob (d) or Ad3 knob (e) (see also Supplementary Figs. 1f and g). Solubilized HeLa cell membrane lysates were also immunoprecipitated with DSG2 mAb 6D8 crosslinked with protein A/G plus agarose. Western blot of immunoprecipitates was performed with DSG2 monoclonal antibody AH12.2 (see antiDSG2-IP). **f)** MS/MS analysis of the 160 kDa band. Upper panel: Structure of DSG2. EC: extracellular domain, EA: juxtamembrane extracellular anchor domain, TM: transmembrane domain. Lower panel: amino acid sequence of DSG2. Highlighted are the peptide sequences captured by MS/MS analysis of the 160 kDa band. The triangles in the DSG2 scheme (top panel) indicate the localization of the identified peptides with regards to the different domains. MS/MS analysis detected 14 peptides DSG2 with a high confidence factor (20.8% protein coverage and Sequest cross correlation coefficient scores ranging from 2.6 to 5.5 for individual peptides). **g–i)** Biacore plasmon surface resonance studies with recombinant human DSG2 immobilized on sensorchips. Ad2, Ad3 and Ad5 at 5.10^{9} vp per ml (g), different concentrations of PtDd (h) or PtDd and Ad3 fiber knob (i) were injected over the activated surface and response signals were collected over the indicated time periods.

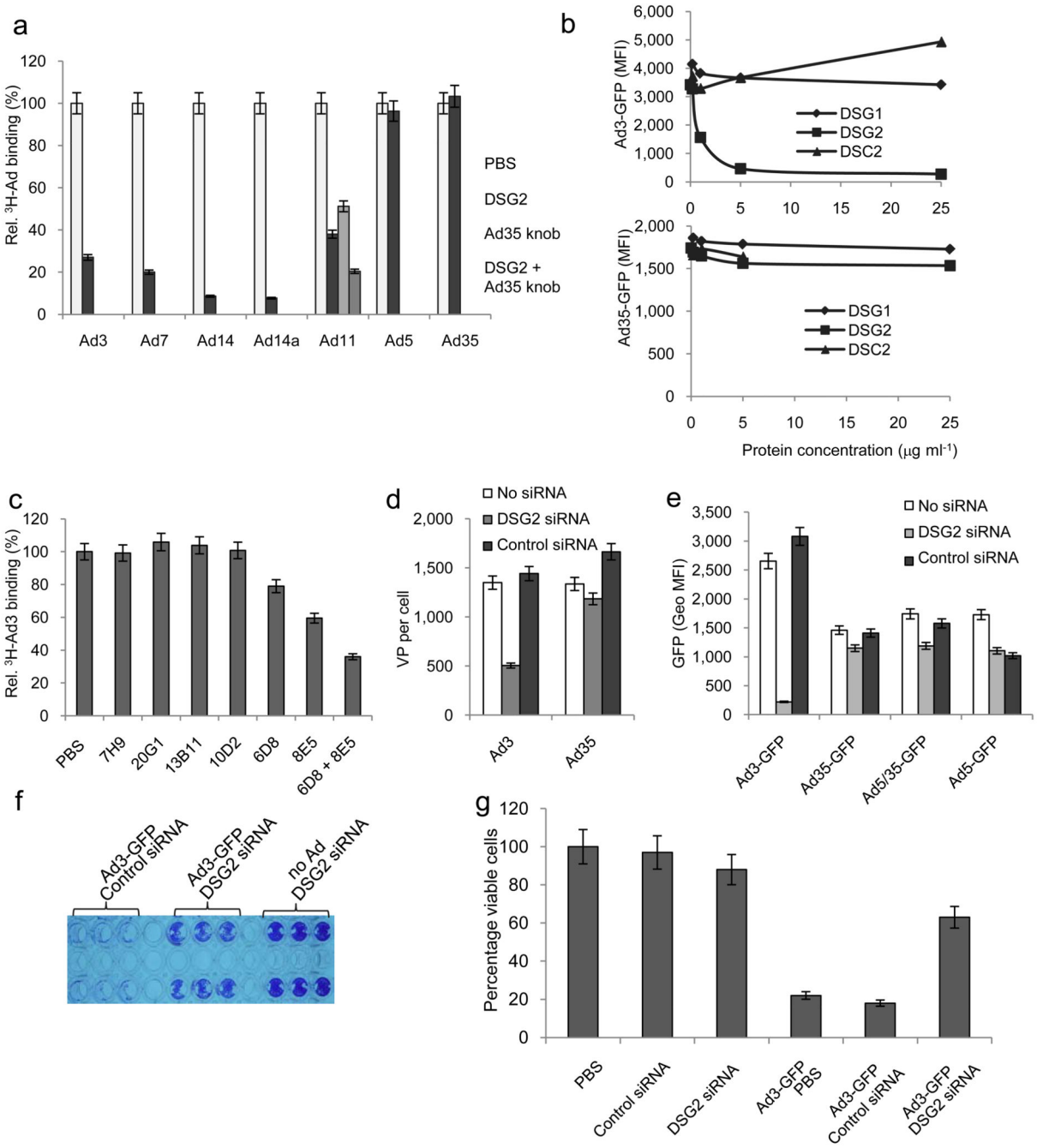

Fig.2. Validation of DSG2 as Ad receptor. "Loss-of-function" studies

a) Competition of ^{3}H-labeled Ad binding by recombinant DSG2. ^{3}H-Ad3, Ad7, Ad14, Ad14a, Ad11, Ad5 and Ad35 virus were pre-incubated with 6 μg ml^{-1} recombinant human DSG2 protein. Attachment of virus particles incubated with PBS was taken as 100%. For analysis of Ad11 attachment, cells were also incubated with 50 μg ml^{-1} of Ad35K on ice for one hour before adding of Ad11 virus to block CD46. **b)** Competition of Ad transduction by recombinant DSG1, DSG2 or DSC2 proteins. **c)** Competition of ^{3}H-Ad binding by DSG2-specific antibodies. *n*=5. PBS vs. 6D8: *P*=0.013; PBS vs. 8E5: *P*=0.0014. The specificity of

mAbs to different DSG2 domains is as follows (for a scheme of DSG2, see Supplementary Fig. 1f): 20G1 (Pro-peptide region), 7H9 (Pro/EC1), 13B11 (EC1/EC2), 10D2 (EC1/EC2), 8E5 (EC3), 6D8 (EC3/EC4). **d) and e)** Effect of siRNA-mediated DSG2 downregulation on Ad attachment (d) and transduction (e). Shown are mean fluorescence intensity values. n=5. Note that at 18 hours post-infection, GFP levels were comparable for Ad35-GFP and Ad5/35-GFP, which allowed us to also use the first-generation Ad5/35-GFP vector in further studies. **f)** Cytolysis of Ad3-GFP infected BT474 cells at day 7 after infection. siRNA transfected cells were infected at adjusted MOIs that allow for comparable initial transduction rates, i.e. MOI 1.0 pfu per cell and 0.5 pfu per cell for DSG2 siRNA and control siRNA treated cells, respectively. Seven days later, viable cells were stained with crystal violet. Despite the higher virus dose, less killing was seen in cells transfected with DSG2 siRNA, suggesting the importance of DSG2 in lateral spreading of Ad3. **g)** Cytolysis of Ad3-GFP infected cells at day 7 after infection. siRNA transfected small airway epithelial cells were infected at adjusted MOIs. Seven days later, cell viability was measured by WST-1 assay. Viability of PBS treated cells was taken 100%. n=3. Ad3-GFP/control siRNA vs. Ad3-GFP DSG2 siRNA: P<0.001.

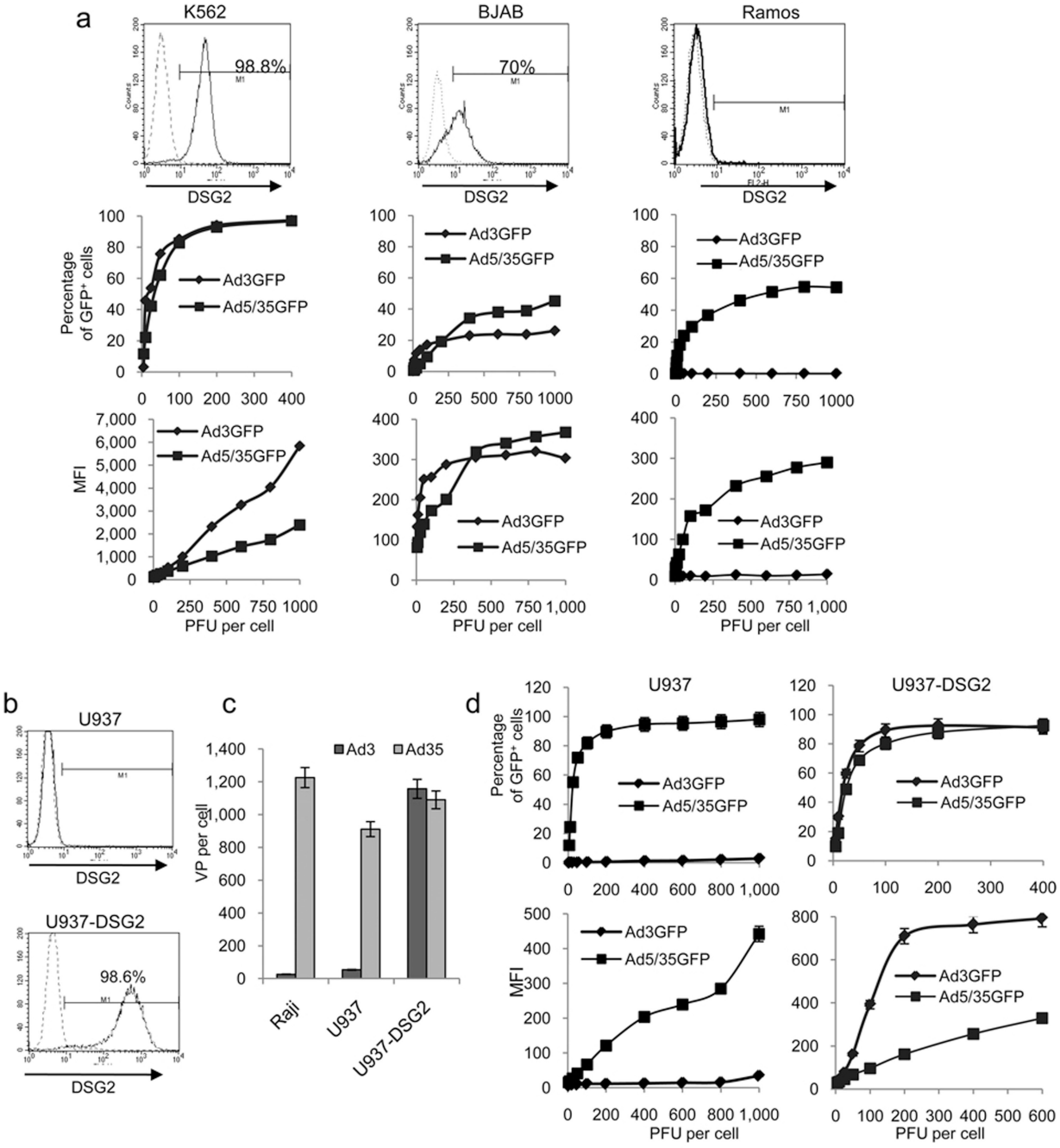

Fig.3. Validation of DSG2 as Ad receptor. "Gain-of-function" studies

a) Transduction of human cell lines that express different DSG2 levels. Human erythromyeloblastoid leukemia K562 cells and Burkitt's B-cell lymphoma BJAB and Ramos cells were infected with Ad3-GFP and Ad5/35-GFP at increasing MOIs and GFP expression was measured 18 hours later. N=3. Standard deviation was less than 10% for all data points. **b)** Ectopic DSG2 expression. Human histiocytic lymphoma U937 cells were infected with a lentivirus vector carrying the DSG2 cDNA under the control of the EF1α promoter. Stable DSG2 expression was detected in >98% of lentivirus transduced cells by flow cytometry. **c)**

Attachment of ^{3}H-Ad3 and ^{3}H-Ad35 to Raji, U937 and DSG2-expressing U937 (U937-DSG2) cells. Note that Ad35 attachment is mediated through CD46 and can be blocked by soluble CD46 (data not shown). **d)** GFP expression after transduction of U937 and U937-DSG2 cells with Ad3-GFP and Ad5/35-GFP. *n*=3

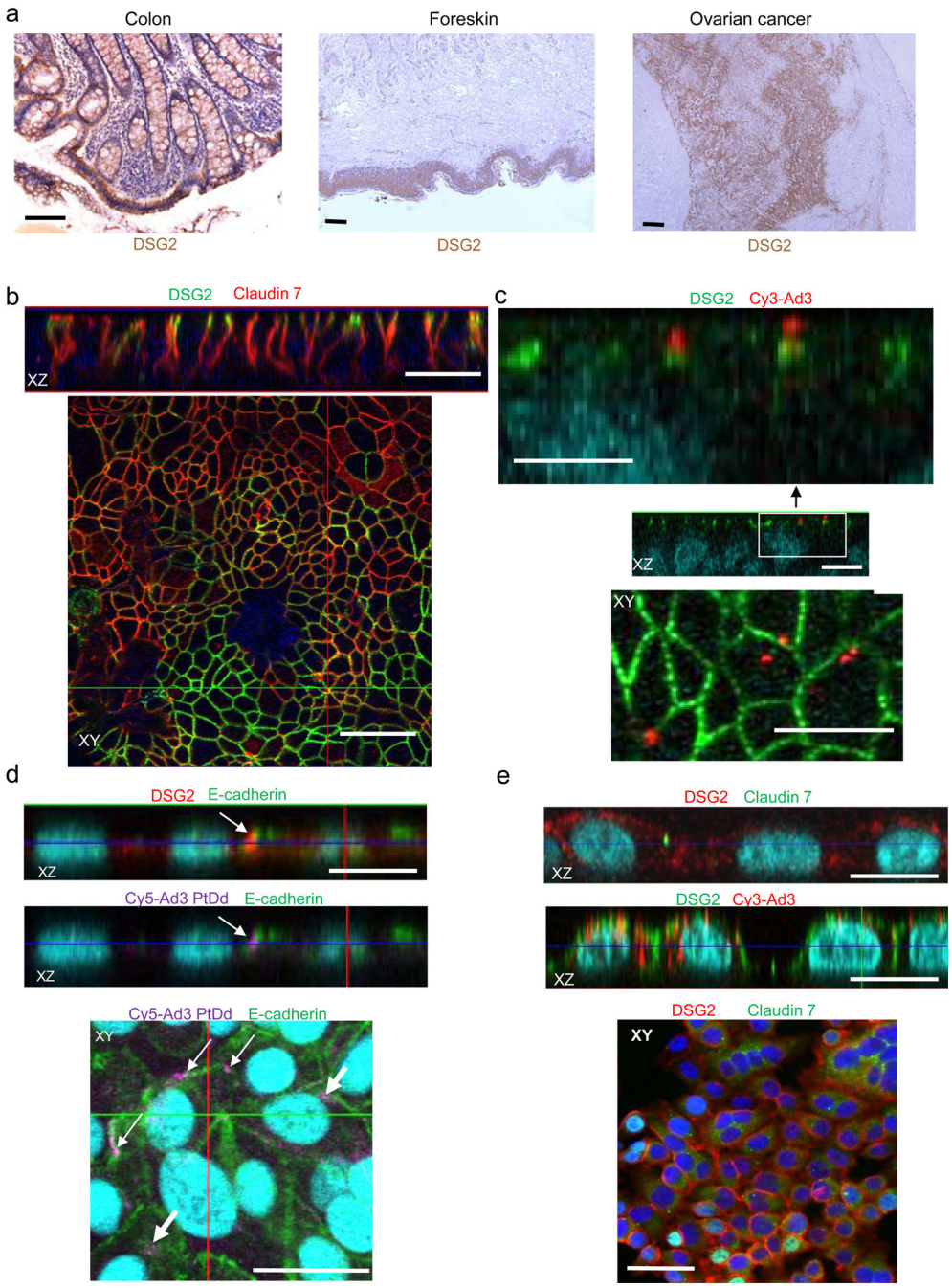

Fig.4. DSG2 localization in human epithelial cells and interaction with Ad3

a) Immunohistochemistry studies on human colon, foreskin and ovarian cancer paraffin sections with DSG2-specific antibodies. Positive staining appears in brown. **b)** Confocal microscopy immunofluorescence analysis of polarized human colon cancer T84 cells for DSG2 (green) and the intercellular junction protein Claudin 7 (red). Nuclei are blue. XY and XZ planes are shown. **c)** Ad3 binding to DSG2. T84 cells were incubated with Cy3-labeled Ad3 particles (red) for 15 minutes, washed, and subjected to confocal microscopy. The upper XZ image is a higher magnification. Note that at least two (green) DSG2 signals are

associated with one (red) Cy3-Ad3 signal. **d)** Confocal microscopy of normal human small airway epithelial cells (not grown in Transwell chambers). Cells were incubated with Cy5-labelled PtDd for 15 min and then washed with PBS. The upper XZ panel shows co-localization of DSG2 (red) and E-cadherin (green). The lower XZ panel is the same image showing purple Cy5-PtDd signals co-localized with green E-cadherin signals. The XY panel shows purple (PtDd) and green E-cadherin channels. Thin arrows mark membrane localized PtDd, thick arrows label cytoplasmic DSG2. **e)** Confocal microscopy immunofluorescence analysis of human cervical carcinoma HeLa cells (upper XZ and XY panels) and HeLa cells incubated for 15 min with Cy3-Ad3 (lower XZ panel).
Scale bars for all confocal microphotographs are 20 μm.

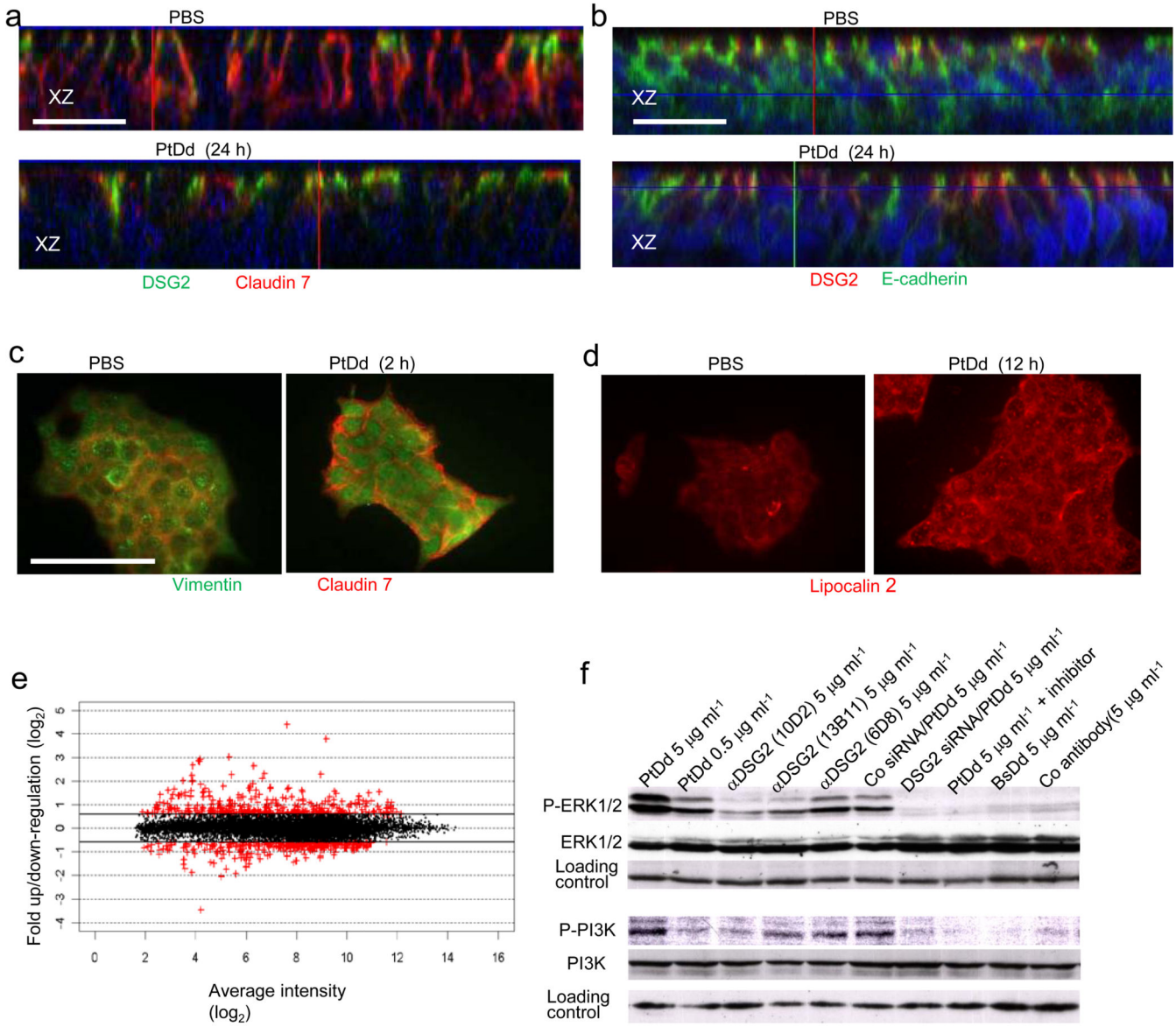

Fig.5. Epithelial-to-mesenchymal transition signaling induced by Ad3 virions and PtDd in epithelial cells

a–d) Phenotypic changes triggered by PtDd in breast cancer epithelial cells. 1×10^5 BT474 cells were incubated with 50 ng of PtDd or BsDd for the indicated time and subjected to staining with antibodies. The scale bar is 20 µm in all ZY confocal images (a, b) and 40 µm in the standard immunofluorescense studies (c, d). **e)** Graphic demonstration of array data for up- and down-regulated genes (PtDd vs. PBS treated cells). Each dot represents one gene. **f)** Western blot analysis of ERK1/2-MAPK and PI3K phosphorylation analyzed 6 hours after incubation of BT474 cells with PtDd, BsDd, DSG2-specific antibodies (10D2, 13B11, or 6D8), or control antibody (anti-GAPDH) at the indicated concentrations. For pathway inhibition, cells were treated overnight with Erk1/2 inhibitor UO126 (5 µM) or PI3K inhibitor Wortmannin (2.5 µM) before PtDd was added. The efficacy of the drugs for

inhibition of the specific pathway was validated in a previous study 8. GAPDH is used to demonstrate equal loading.

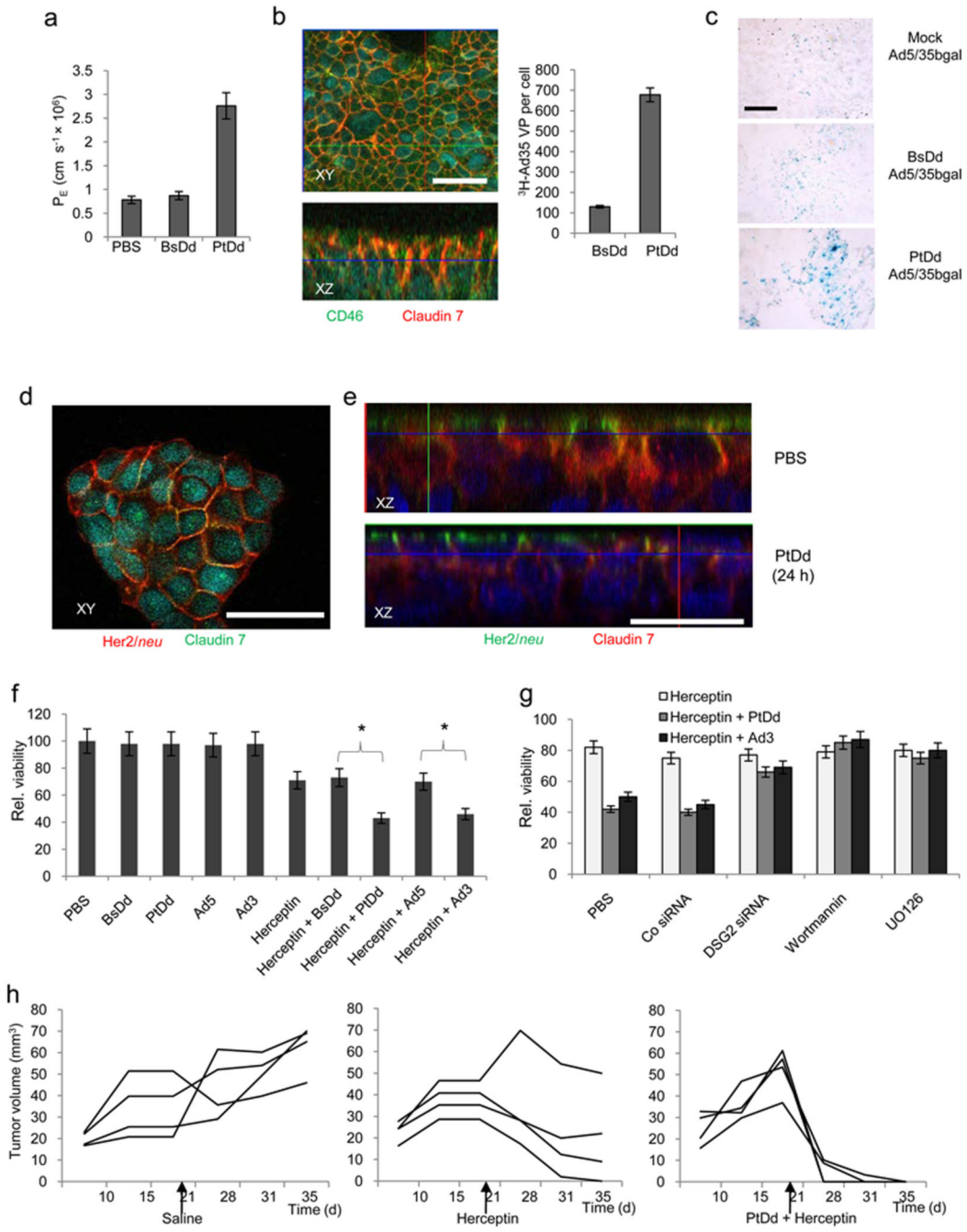

Fig.6. Opening of intercellular junctions in epithelial breast cancer cells by interaction of Ad3 virions or PtDd with DSG2

a) FITC-Dextran diffusion through monolayers of BT474 cells. BT474 cells cultured in transwell chamber with 0.4 μm pore size were treated with 0.5 μg ml^{-1} BsDd, PtDd or 2×10^8 Ad particles per ml for 2 hours and then 4 kDa FITC-dextran was added to the apical compartment. Paracellular flux was assessed in aliquots from the apical and basal chambers. BsDd vs. PtDd: $P<0.001$. **b)** Facilitation of ^{3}H-Ad35 uptake by PtDd. Left panel: Trapping of CD46 in intercellular junctions of T84 cells. Co-localization of CD46 and the intercellular

junction protein Claudin 7 results in yellow signals. Right panel: ^{3}H-Ad35 attachment. BT474-cells were incubated with PtDd or BsDd and ^{3}H-Ad35 for 2 hours on ice, washed, and then incubated at 37°C for 60 min. Non-internalized Ad particles were removed by trypsin digestion and cell-associated radioactivity was measured. **c)** Mice carrying subcutaneous ovc316 tumors were injected intravenously with 50 μg PtDd or BsDd eight hours before intravenous injction of 1×10^{9} pfu of Ad5/35-bGal. Sections were stained with X-gal 72 hours after injection. The scale bar is 40 μm. **d)** Confocal microscopy for Her2/*neu* and Claudin 7 in the Her2/*neu*-positive human breast cancer cell line BT474. These cells do not form monolayers. Note that in PBS treated cells, most Her2/*neu* signals (green) colocalize with Claudin 7 (red) resulting in yellow signals. Upon PtDd treatment, Claudin 7 signals decrease while more Her2/*neu* staining appears on the cell surface. **e)** Confocal microscopy of BT474 cells two hours after treatment with PBS or PtDd. **f)** Ad3 and PtDd enhance killing of Her2/*neu* positive breast cancer cells by Herceptin. Viability of PBS-treated cells was taken 100%. n=5, *P<0.05. **g)** Ad3 and PtDd enhancement of Herceptin therapy is mediated by DSG2 and involves ERK/MAPK and PI3K pathways. BT474 cells were transfected with control and *DSG2* siRNA as described in Fig. 2d and 48 hours later treated with Ad3 or PtDd and Herceptin as described in g). For inhibitor studies, BT474 cells were incubated with the indicated agents overnight. Cells were washed and treated with PtDd/Ad3 and Herceptin as described in above. n=5, PBS vs. Wortmannin, UO126: P<0.05. **h)** PtDd-mediated enhancement of Herceptin therapy *in vivo*. Shown is the tumor volume of individual mice at different days after BT474-M1 cell injection.